

Strong export of Antarctic Bottom Water east of the Kerguelen plateau

Y. Fukamachi^{1*}, S. R. Rintoul^{2,3,4}, J. A. Church^{2,3,4}, S. Aoki¹, S. Sokolov^{2,3,4}, M. A. Rosenberg⁴ and M. Wakatsuchi¹

The primary paths for the transport of Antarctic Bottom Water from the Southern Ocean into the global ocean are the deep western boundary currents east of the Antarctic Peninsula and the Kerguelen plateau¹. Previous ship-based observations documented distinct water properties and velocities associated with a deep western boundary current in the Kerguelen region^{2–7}, but the mean flow is as yet unconstrained. Here we report measurements from a coherent array of eight current-meter moorings that reveal a narrow and intense equatorward flow extending throughout the water column just east of the Kerguelen plateau. Velocities averaged over two years exceed 20 cm s^{-1} at depths of about 3,500 m, the strongest mean deep western boundary current flow yet observed at similar depths. We estimate the mean equatorward transport of water colder than 0°C at $12.3 \pm 1.2 \times 10^6 \text{ m}^3 \text{ s}^{-1}$, partially compensated by poleward flow. We also estimate the net equatorward flow of water colder than 0.2°C at about $8 \times 10^6 \text{ m}^3 \text{ s}^{-1}$, substantially higher than the $1.9 \times 10^6 \text{ m}^3 \text{ s}^{-1}$ reported from the boundary current that carries dense water from the Weddell Sea into the Atlantic Ocean north of the Falkland plateau⁸. We conclude that the Kerguelen deep western boundary current is a significant pathway of the global ocean's deep overturning circulation.

The global overturning circulation is the dominant mechanism responsible for oceanic heat transport as a result of the large temperature difference between the upper and lower limbs of the overturning cell. The overturning circulation thus has a strong influence on climate. The deep branch of the overturning circulation is supplied by cold, dense water formed in the high-latitude North Atlantic Ocean and the Southern Ocean and exported from the formation regions in a global network of deep western boundary currents (DWBCs), partially compensated by recirculation gyres and slower flows in the interior of the ocean basins⁹.

Previous estimates suggest that the Weddell Sea provides ~60% of the total 8.1 Sv ($1 \text{ Sv} = 10^6 \text{ m}^3 \text{ s}^{-1}$) of Antarctic Bottom Water (AABW) formed in the Southern Ocean¹, with most of the remainder formed in the Ross Sea and off Adélie Land^{1,10}. The abyssal chlorofluorocarbon distribution shows that AABW is exported to lower latitudes by two DWBCs (ref. 1). The first transports Weddell Sea AABW along the Antarctic Peninsula and South Sandwich Island arc to ventilate the deep waters of the Atlantic Ocean and the western Indian Ocean¹¹. The second transports Ross Sea and Adélie Land AABW equatorward east of the Kerguelen plateau, before passing through fracture zones in the mid-ocean ridge systems to supply the abyssal layers of the eastern Indian and Pacific oceans^{1,5,12} (Fig. 1a). The Kerguelen DWBC also returns the poleward flow carried by a deep cyclonic

gyre in the interior of the Australian Antarctic basin (AAB). The high concentration of chlorofluorocarbons near the sea floor^{1,13} in the AAB indicates that it is the best-ventilated deep basin around Antarctica.

Current-meter moorings have confirmed the presence of a DWBC carrying dense water equatorward in the northwest Weddell Sea^{11,14} and north of the Falkland Islands⁸ (Supplementary Table S1). Ship-based synoptic 'snapshots' have confirmed the presence of a DWBC east of the Kerguelen plateau^{2–7}, but no time-series measurements have been made to allow estimates of its mean flow and variability. To estimate this flow, we deployed an array of eight closely spaced current-meter moorings on the eastern flank of the plateau from February 2003 to January 2005 (Figs 1b and 2). The horizontal coherence and duration of the array allowed accurate estimates of the transport and structure of the Kerguelen DWBC.

The DWBC forms a narrow (~50 km wide), intense, bottom-intensified flow to the northwest over the lower flank of the plateau, with a flow to the southeast further offshore (Fig. 2). The currents are remarkably strong for these depths: maximum two-year mean speed exceeds 20 cm s^{-1} at ~3,500 m depth at M6 (the largest DWBC speeds yet observed at similar depths; Supplementary Table S1), much stronger than measured in the DWBC exporting AABW from the Weddell Sea^{8,11,14}. The mean distribution of potential temperature (θ) shows that AABW (defined as $\theta < 0^\circ \text{C}$ following ref. 15) exists below 2,500 m, forming a layer 1,500 m thick off the continental rise (Fig. 2). Mean near-bottom potential temperatures at M3–5 are ~ -0.35°C . The isotherms slope up to the west with the coldest and thickest AABW layer over the lower flank of the plateau.

Three snapshots of the potential temperature and velocity field obtained from conductivity–temperature–depth (CTD) profiler and lowered acoustic Doppler current profiler (ADCP) sections during the experiment show a similar structure to the mean field derived from the mooring data, confirming the barotropic nature of the DWBC, with northwestward flow extending throughout the water column (an example in ref. 6). The similarity between the moored results and the synoptic snapshots indicates that the limited vertical resolution of the moored instruments is sufficient to capture the DWBC structure.

The daily velocity and potential temperature data are used to calculate the AABW transport per unit width (Fig. 3a). The northwestward transport of AABW is concentrated between M4 and M6, with the largest value observed at M5 where the velocities are large and the AABW layer is thick (Fig. 2). Northwestward transport is commonly observed to extend offshore as far as M3

¹Institute of Low Temperature Science, Hokkaido University, Sapporo 060-0819, Japan, ²Centre for Australian Weather and Climate Research—a partnership of the Bureau of Meteorology and CSIRO, Hobart, Tasmania 7000, Australia, ³Wealth from Oceans Flagship, Hobart, Tasmania 7000, Australia, ⁴Antarctic Climate and Ecosystem Cooperative Research Centre, Hobart, Tasmania 7001, Australia. *e-mail: yasuf@lowtem.hokudai.ac.jp.

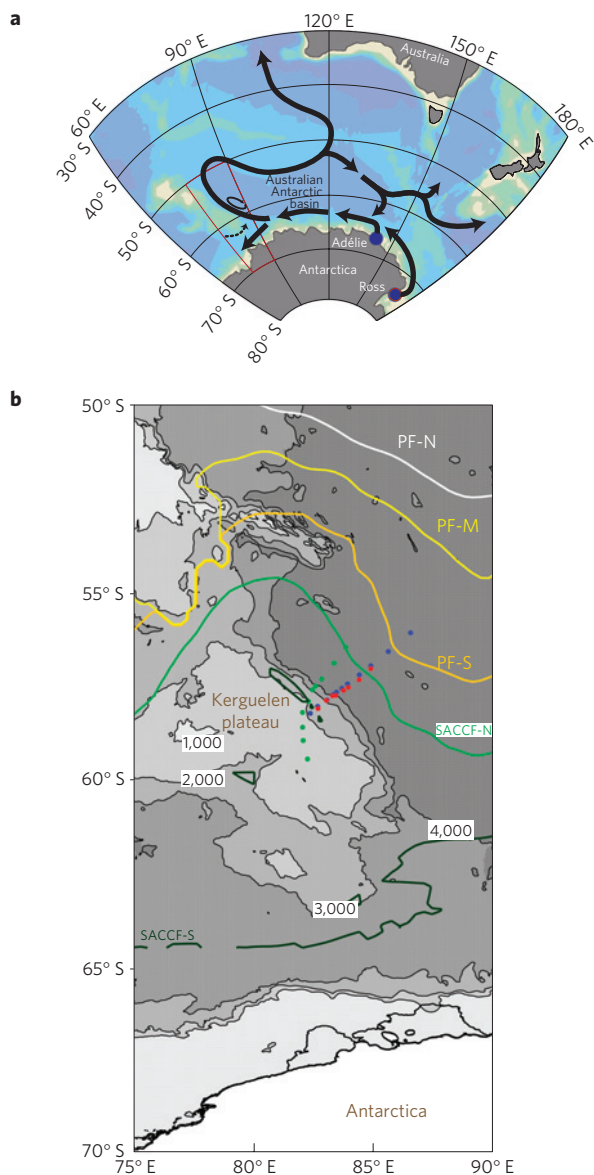


Figure 1 | Maps of the Indian and Pacific sectors of the Southern Ocean and the region around the Kerguelen plateau. **a**, A schematic view of AABW sources and boundary currents carrying AABW. The region in **b** is outlined in red. **b**, Mooring locations (red) and CTD stations used to estimate transport during the WOCE IBS (green, ref. 3) and BEAGLE2003 (blue, ref. 6) cruises. Locations of branches of the Polar Front and the SACC are drawn after ref. 28.

(~38 km from M5) and occasionally as far as M2 (~77 km from M5). A spectral analysis indicates that the DWBC transport is modulated by fluctuations with a period of ~20–40 days, probably reflecting the presence of topographic waves (for example, ref. 16); the magnitude of the fluctuations is largest in the core of the DWBC near the base of the sloping topography and declines offshore. Overall, however, the core of the DWBC is relatively steady in both location and magnitude. The sense of the flow is reversed further offshore, reflecting the presence of the deep expression of branches of the Southern Antarctic Circumpolar Current Front (SACC) and Polar Front (Fig. 1b), which cross the array from northwest to southeast at the eastern end of the array, the cyclonic gyre in the AAB (ref. 5) and possibly a local recirculation⁶.

The total northwestward AABW transport, integrated from the inshore edge of the array (M8) to the zero-crossing point from

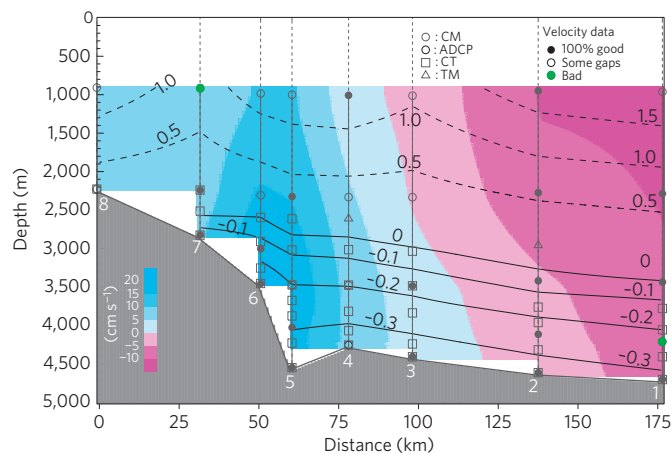


Figure 2 | Mean sections of velocity and potential temperature.

The mean sections of the velocity perpendicular to the mooring array (shading; positive northwestward) and potential temperature (contours) over the entire duration. Also shown is a schematic diagram of moorings. CM, CT and TM denote current meter, conductivity–temperature recorder and thermistor. Ratios of valid velocity data are indicated by three symbols.

northwestward to southeastward flow (see the Methods section), varies from 0.1 to 30.3 Sv (light blue curve, Fig. 3b) around an overall mean value of 12.3 Sv (dark green line), with a standard deviation of 5.6 Sv. The zero-crossing point is generally located just to the south of the northern branch of the SACC and fluctuations in its position correspond to shifts in the front (green curve, Fig. 3a). Variability with timescales of ~20–40 days is clearly dominant, but lower frequency variability is also observed and largely reflects the influence of eddies and fronts of the Antarctic Circumpolar Current (ACC; as seen in satellite altimeter data, not shown). For example, the northwestward transport of AABW is briefly reduced to values less than 2 Sv on four occasions, each of which coincides with onshore translations of the ACC fronts or eddies (Fig. 3). Maxima in transport are observed when the presence of a cyclonic eddy over the eastern side of the array reinforces the northwestward flow. There is little evidence of seasonal variability. Despite the energetic variability, the mean flow is well defined and the 95% confidence intervals (with the de-correlation time of 8.5 days) are narrow (± 1.2 Sv). The cumulative average of the transport estimates (green curve) is within the 95% confidence intervals of the mean after nine months, indicating that the records are of sufficient length to establish a stable mean. The overall impression is of a narrow, intense and relatively steady deep boundary current, modulated by topographic waves and the episodic influence of fronts and meanders of the ACC. This DWBC is associated with a mean temperature transport of -2.52 ± 0.26 Sv °C northwestward.

Snapshot estimates based on CTD/ADCP measurements are in agreement with the observations from the moored array, with the exception of the deployment cruise (Fig. 3b, Supplementary Table S2). However, these estimates sampled periods of larger than average transport (Fig. 3b) and hence give a larger and misleading impression of the strength of the mean flow. Long time series are essential to determine robust mean values of variable ocean currents such as the Kerguelen DWBC.

The southeastward flow across the eastern end of the array returns some AABW to the south. Integrating northeastwards from M8 and including the southeastward transport, the mean net northwestward transport of AABW reaches a maximum of 10.3 Sv (with a standard deviation of 4.7 Sv) at M3 and is 6.8 Sv across the entire array (standard deviation 7.9 Sv) (Fig. 3c). The southeastward flow reflects deep flow associated with the ACC and local⁶ or basin-scale⁵ recirculations; a portion of this flow

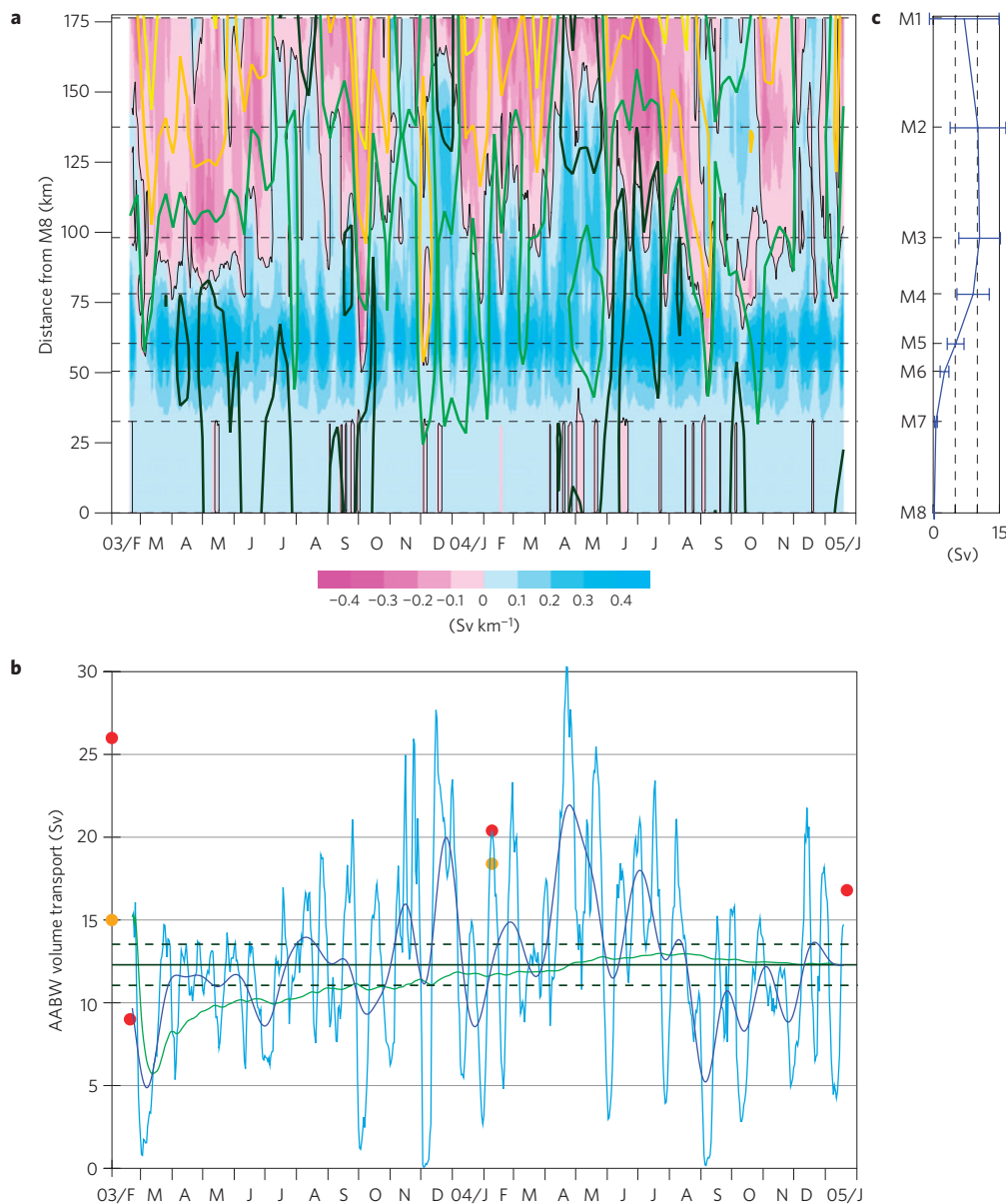


Figure 3 | AABW transport. **a**, Daily transport per unit width (Sv km^{-1}); positive northwestward (blue). ACC fronts are shown in the same colours as in Fig. 1b. **b**, Daily (light blue) and low-passed volume transport (dark blue, 40-day Butterworth filter). Cumulative mean (green) and overall mean (dark green) with 95% confidence limit (dark green dashed). The dots are snapshot estimates from hydrographic sections referenced to shipboard (orange) and lowered (red) ADCP data. Estimates from WOCE in 1994–1995 (ref. 3) are shown on the left axis. **c**, Cumulative net AABW volume transport from M8 (curve) and standard deviation (bars).

may turn back to the north, east of the array^{5,6}. Recirculation gyres offshore of DWBCs are predicted by theory⁹ and frequently observed^{17–20}, and make it difficult to estimate the net throughflow of the deep overturning circulation¹⁷. Property distributions show that recently ventilated AABW carried north in the DWBC exits the basin through fracture zones in the ridge to supply the deep southeast Indian Ocean, the Tasman Sea and the Pacific Ocean⁵. However, there are no quantitative estimates of the mean export of AABW through the fracture zones.

Several factors make it difficult to assess the relative contribution of the Kerguelen DWBC to the Southern Ocean overturning. These include the presence of recirculation gyres, interaction between the DWBC and other circulation regimes (for example, the ACC and subpolar gyres)⁸, the fact that mixing and entrainment change the volume and properties of AABW along the export pathway¹³ and the lack of coherent long-term observations in other DWBCs. The only

previous coherent current-meter measurements of AABW export by a DWBC south of 45°S were obtained north of the Falkland plateau, where a net transport of 1.9 Sv of Weddell Sea Deep Water ($\theta < 0.2^\circ\text{C}$) was found to enter the Argentine basin (the difference between 8.2 Sv westward and 6.3 Sv recirculating to the east⁸). In comparison, the net transport of water with $\theta < 0.2^\circ\text{C}$ by the Kerguelen DWBC is 8.0 Sv (16.4 Sv to the northwest and an 8.4 Sv recirculation to the southeast). Incoherent multi-year moored measurements in the northwest Weddell Sea reveal relatively weak currents (deep mean flows $< 7\text{ cm s}^{-1}$; ref. 11). Combining these current-meter data with CTD sections gives a net export of 3.8 Sv of AABW ($\theta < 0^\circ\text{C}$) from the Weddell Sea¹⁴; on the basis of an inverse model, a further 4.7 Sv may leave the Weddell Sea across the Scotia ridge²¹. Estimates of AABW ($\theta < 0^\circ\text{C}$) export from the Weddell Sea derived from alternative approaches (for example, mass and tracer budgets or inverse models) vary by a factor of three (from

3.3 to 10.0 Sv; ref. 21). Although the lack of long-term, coherent velocity measurements spanning the boundary current and offshore recirculations makes it difficult to be definitive about the relative size of the Atlantic and Kerguelen DWBCs, we can conclude that the two are at least comparable in magnitude.

Recognition of the importance of the overturning circulation in the climate system and its potential vulnerability has driven enhanced efforts to obtain long-term measurements of the DWBC system in the North Atlantic (for example, the RAPID/MOCHA programme^{22–24}). The Southern Ocean limb of the overturning ventilates the deep ocean at about the same rate as the North Atlantic¹³, is dynamically coupled to the Atlantic overturning²⁵ and is also potentially sensitive to future climate change^{26,27}. An understanding of the global overturning circulation and its response to changes in forcing therefore requires an observing system that provides sustained measurements of the main pathways of the overturning circulation in both hemispheres. Our results show that the Kerguelen DWBC is one of these main pathways. The demonstration that robust transport estimates can be made with simple, coherent arrays of current-meter moorings provides a guide to the type of sustained measurements needed at this and other locations in the Southern Ocean.

Methods

Eight moorings containing 31 current meters (Aanderaa RCM-5 and 8), 2 ADCPs (RD Instruments WH-Sentinel 300 kHz), 33 conductivity–temperature recorders (SeaBird SBE 37) and 2 thermistors (SeaBird SBE 39) were deployed and recovered by RSV *Aurora Australis* in February 2003 and January 2005 (Fig. 2). Valid data were obtained by most of the instruments; instruments with gaps are indicated in Fig. 2. Top-to-bottom temperature and salinity profiles were taken by a CTD profiler (SeaBird SBE 911plus) during the deployment and recovery cruises and the BEAGLE2003 cruise by RV *Mirai* in February 2004. Near-surface and full-depth velocity data taken by shipboard (RDI broadband 75 kHz) and lowered (RD Instruments WH-Sentinel 300 kHz) ADCPs during the BEAGLE2003 cruise are used. Near-surface and full-depth velocity data taken by shipboard (RDI narrowband 150 kHz) and lowered ADCPs (SonTek ADP 250 kHz) during the deployment and recovery cruises are also used.

Instrument depths are estimated using pressure values measured by the current meters (mostly second instrument from the top) and assuming that moorings remained straight although with tilt. (Nominal instrument depths are used during the entire mooring period at M8 because of the failed pressure sensor.) For the water column above the uppermost conductivity–temperature recorder at each mooring, temperature data from current meters and thermistors are used. These temperature data are converted to potential temperature (the temperature of the water parcel if it was raised adiabatically to the surface) using the average salinity at the same pressure among the three CTD observations in February 2003 and 2004 and January 2005. For the water column below the uppermost conductivity–temperature recorder, potential temperature values derived at conductivity–temperature recorders are only used. Note that the assumption of nominal instrument depths at M8 and the use of potential temperature data converted with the average CTD data have minimal effects on the resulting AABW volume transport estimate because AABW mostly exists below 2,500 m and away from M8 (Fig. 2). Two-hourly data of velocity perpendicular to the mooring array and potential temperature were calculated in 10-m vertical bins between depths of 900 m and the bottom, mostly by interpolation and slightly by extrapolation above (below) the uppermost (lowermost) valid data.

Using these vertically binned data at each mooring and cross-sectional areas between adjacent moorings, daily AABW volume transports ($\theta < 0^\circ\text{C}$) are calculated by integrating from M8 over the slope to the zero-crossing point from the northwestward to southeastward transport (Fig. 3). Estimation of the net AABW transport is complicated by several factors, including the presence of recirculation gyres, upper ocean currents (for example, fronts of the ACC) opposing or enhancing the deep flow and synoptic variability such as eddies and frontal meanders. Integrating to the zero-crossing point, as done here, is a commonly used approach (for example, ref. 17) that permits comparison to other studies, but remains arbitrary. The coincidence of the zero-crossing point with the location of the northern branch of the SACCF, which carries AABW to the southeast, provides further oceanographic support for choosing the zero-crossing point as the offshore edge of the DWBC. We explored several alternative methods of integrating the AABW transport. The time mean of the sum of all northwestward flow of AABW across the array gives 12.9 Sv (compared with 12.3 Sv inshore of the zero-crossing point). The difference in the mean between this northwestward flow and the sum of all the southeastward flow (6.0 Sv) is the net northwestward flow (6.8 Sv) across the array. Using the mean velocity and potential temperature sections, and integrating

northwestward flows to the zero-crossing point, gives 10.4 Sv. (The difference between estimates using the mean fields and the full time series reflects the fact that both the area and velocity of the AABW layer differ in the two cases, in part because the mean field includes periods of southeastward flow.) The AABW transports from ref. 6 shown in Fig. 3b and Supplementary Table S2 were re-calculated using a potential temperature of 0°C to define AABW.

The locations of the ACC fronts (Figs 1b and 3a) are identified as specific values of the absolute sea surface height field (for example, ref. 28). The sea surface height field is derived from the combination of CLS/AVISO 'Mean Sea Level Anomaly' maps, which are produced by mapping data from the TOPEX/POSEIDON, ERS-1 and ERS-2 satellite altimeters²⁹, and the mean dynamic height data from the climatology of ref. 30.

Received 29 October 2009; accepted 15 March 2010;
published online 25 April 2010

References

- Orsi, A. H., Johnson, G. C. & Bullister, J. L. Circulation, mixing, and production of Antarctic Bottom Water. *Prog. Oceanogr.* **43**, 55–109 (1999).
- Speer, K. G. & Forbes, A. A deep western boundary current in the South Indian basin. *Deep-Sea Res. I* **41**, 1289–1303 (1994).
- Donohue, K., Hufford, G. E. & McCartney, M. S. Sources and transport of the deep western boundary current east of the Kerguelen plateau. *Geophys. Res. Lett.* **26**, 851–854 (1999).
- Narumi, Y., Kawamura, Y., Kusaka, T., Kitade, Y. & Nagashima, H. The Deep Western Boundary Current along the eastern slope of the Kerguelen plateau in the Southern Ocean: Observed by the Lowered Acoustic Doppler Profiler (LADCP). *La Mer* **43**, 49–59 (2005).
- McCartney, M. S. & Donohue, K. A. A deep cyclonic gyre in the Australian–Antarctic basin. *Prog. Oceanogr.* **75**, 675–750 (2007).
- Aoki, S. *et al.* Deep western boundary current and southern frontal systems of the Antarctic Circumpolar Current southeast of the Kerguelen Plateau. *J. Geophys. Res.* **113**, C08038 (2008).
- Park, Y.-H., Vivier, F., Roquet, F. & Kestenare, E. Direct observations of the ACC transport across the Kerguelen plateau. *Geophys. Res. Lett.* **36**, L18603 (2009).
- Whitworth, T. III, Nowlin, W. D., Pillsbury, R. D., Moore, M. I. & Weiss, R. F. Observations of the Antarctic Circumpolar Current and deep boundary current in the Southwest Atlantic. *J. Geophys. Res.* **96**, 15105–15118 (1991).
- Stommel, H. & Arons, A. B. On the abyssal circulation of the World Ocean—I. Stationary planetary flow patterns on a sphere. *Deep-Sea Res.* **6**, 140–154 (1960).
- Rintoul, S. R. in *Ocean, Ice, and Atmosphere: Interactions at the Antarctic Continental Margin* (eds Jacobs, S. S. & Weiss, R. R.) 151–171 (Antarct. Res. Ser., Vol. 75, American Geophysical Union, 1998).
- Fahrbach, E., Harms, S., Rohardt, G., Schröder, M. & Woodgate, R. A. Flow of bottom water in the northwestern Weddell Sea. *J. Geophys. Res.* **106**, 2761–2778 (2001).
- Nakano, H. & Sugimoto, N. Importance of the eastern Indian Ocean for the abyssal Pacific. *J. Geophys. Res.* **107**, 3219 (2002).
- Orsi, A. J., Smethie, W. M. Jr & Bullister, J. L. On the total input of Antarctic waters to the deep ocean: A preliminary estimate from chlorofluorocarbon measurements. *J. Geophys. Res.* **107**, 3122 (2002).
- Fahrbach, E., Rohardt, G., Schröder, M. & Strass, V. Transport and structure of the Weddell Gyre. *Ann. Geophys.* **12**, 840–855 (1994).
- Carmack, E. C. in *Voyage of Discovery* (ed. Angel, M.) *Deep-Sea Res.* **24** (suppl.), 15–37 (1977).
- Moore, M. I. & Wilkin, J. L. Variability in the South Pacific Deep Current from current meter observations and a high-resolution global model. *J. Geophys. Res.* **103**, 5439–5457 (1998).
- Schott, F. A. *et al.* Circulation and deep-water export at the western exit of the subpolar north Atlantic. *J. Phys. Oceanogr.* **34**, 817–842 (2004).
- Bryden, H. L., Johns, W. E. & Saunders, P. M. Deep western boundary current east of Abaco: Mean structure and transport. *J. Mar. Res.* **63**, 35–57 (2005).
- Schott, F. A., Fisher, J., Dengler, M. & Zantopp, R. Variability of the Deep Western Boundary Current east of the grand banks. *Geophys. Res. Lett.* **33**, L21507 (2006).
- McCartney, M. S. Recirculating components of the deep boundary current of the northern North Atlantic. *Prog. Oceanogr.* **29**, 283–383 (1992).
- Naveira Garabato, A. C., McDonagh, E. L., Stevens, D. P., Heywood, K. J. & Sanders, R. J. On the export of Antarctic Bottom Water from the Weddell Sea. *Deep-Sea Res. II* **49**, 4715–4742 (2002).
- Cunningham, S. A. *et al.* Temporal variability of the Atlantic meridional overturning circulation at 26.5°N . *Science* **317**, 935–938 (2007).
- Kanzow, T. *et al.* Observed flow compensation associated with the MOC at 26.5°N in the Atlantic. *Science* **317**, 938–941 (2007).
- Johns, W. E. *et al.* Variability of shallow and deep western boundary currents off the Bahamas during 2004–05: Results from 26°N RAPID-MOC array. *J. Phys. Oceanogr.* **38**, 605–623 (2008).

25. Weaver, A. J., Saenko, O. A., Clark, P. U. & Mitrovica, J. X. Meltwater pulse 1 A from Antarctica as a trigger of the Bølling–Allerød warm interval. *Science* **299**, 1709–1713 (2003).
26. Meehl, G. A. *et al.* in *IPCC Climate Change 2007: The Physical Science Basis. Contribution of Working Group I to the Fourth Assessment Report of the Intergovernmental Panel on Climate Change* (eds Solomon, S. *et al.*) (Cambridge Univ. Press, 2007).
27. Sen Gupta, A. *et al.* Projected changes to the Southern Hemisphere ocean and sea ice in the IPCC AR4 climate models. *J. Clim.* **22**, 3047–3078 (2009).
28. Sokolov, S. & Rintoul, S. R. Circumpolar structure and distribution of the Antarctic Circumpolar Current fronts: 1. Mean circumpolar paths. *J. Geophys. Res.* **114**, C11018 (2009).
29. Le Traon, P., Nadal, F. & Ducet, N. An improved mapping method of multisatellite altimeter data. *J. Atmos. Ocean. Technol.* **15**, 522–534 (1998).
30. Gouretski, V. V. & Koltermann, K. P. *WOCE Global Hydrographic Climatology*. A Technical Report, 35 (Berichte des BSH, 2004).

Acknowledgements

We are deeply indebted to D. McLaughlan and K. Miller for their mooring works. Thanks are extended to the officers, crew and scientists on board RSV *Aurora Australis* for their

help with field observations. Discussions with G. Mizuta and Y. Kashino were helpful. Figure 1a was drawn by L. Bell and K. Kitagawa. Other figures were produced by the PSPLOT library written by K. E. Kohler. In Japan, support was provided by Grants-in-Aid 14403006, 17340138, 20244075, 20540419 and 21310002 for Scientific Research from Ministry of Education, Science, Sports and Culture. In Australia, support was provided by the Cooperative Research Centre program of the Australian government and by the Australian National Antarctic Research Expeditions; this work is a contribution to the Australian Climate Change Science Program, funded jointly by the Department of Climate Change, the Bureau of Meteorology and CSIRO.

Author contributions

J.A.C., M.W., S.R.R. and Y.F. planned the experiment; M.A.R., Y.F., S.R.R., J.A.C., S.A. and S.S. carried out the observations; Y.F., M.A.R., S.S. and S.A. carried out data processing; Y.F., S.R.R., J.A.C., S.S. and M.W. wrote the manuscript, with other authors commenting.

Additional information

The authors declare no competing financial interests. Supplementary information accompanies this paper on www.nature.com/naturegeoscience. Reprints and permissions information is available online at <http://npg.nature.com/reprintsandpermissions>. Correspondence and requests for materials should be addressed to Y.F.